THE PUBLISHING HOUSE
OF THE ROMANIAN ACADEMY

PROCEEDINGS OF THE ROMANIAN ACADEMY, Series A,
Special Issue/2018, pp. 183–188

GEOMETRIC OPTIMIZATION OF A TUBE BANK HEAT EXCHANGER IN A SLOW MOVING FREE STREAM

Alex J. FOWLER

University of Massachusetts Dartmouth
Mechanical Engineering Department
North Dartmouth, MA, USA

Corresponding author: Alex FOWLER, E-mail: afowler@umassd.edu

Abstract. This paper reports the results of a computational optimization study performed on a tube bank heat exchanger that is immersed in a low velocity free stream. The stream in this work is unconstrained such that the fluid flow that is intended to provide cooling or heating to the tube bank may be diverted away from the heat exchanger by the presence of the tube bank itself – that is the fluid may pass around the outside of the tube bank rather than through it due to pressure increases that may occur at the entry region of the tube bank. In the low Reynolds number flow regime it is shown that this effect can be significant. Optimization is performed using finite element simulations of incompressible flow through tube banks subject to a maximum volume constraint. Optimization parameters include tube diameter, tube number and the geometric position of the tubes within the specified volume. It is shown that geometric optimization in this regime leads to heat exchanger geometries in which the positioning of the tubes in the entrance region results in increased flow capture within the heat exchanger volume. Such geometric arrangements are shown to lead to increases in heat transfer rates of 20% or more relative to traditional geometric arrangements.

Key words: Heat exchanger, Optimization, Computational heat transfer.

1. INTRODUCTION

This paper presents preliminary studies aimed at determining the optimum geometry for a heat exchanger such that it maximizes heat transfer to the surrounding fluid when subject to a volume constraint. The new aspect of the current work relative to earlier studies is that in this work the heat exchanger is assumed to occupy a space in which the fluid flow that bathes the heat exchanger is free to bypass the heat exchanger as a result of pressure increases caused by the presence of the heat exchanger itself.

Optimization of heat exchangers became of increased interest in the 1990's with the advent of high performance computer chips that needed to be cooled within tight volume constraints. The demand for increased cooling density has led to the exploration and development of many new cooling technologies such as micro-heat sinks, heat pipes and micro-channel cooling [1], but an interest also developed in determining the optimal geometries for classic heat exchanger designs.

Extensive studies aimed at the geometric optimization of shell and tube, plate and counterflow heat exchangers have been undertaken in which up to seven different geometric design variables have been used to optimize heat exchangers for minimum operating cost, minimum entropy generation, minimum exergy destruction, minimum volumes and other criteria [2–16]. In all of these studies, however, the fluid in the flow field is forced through the heat exchanger. Pressure drop in the fluid is often included either indirectly as it affects operating costs or directly as a parameter, but the flow in these systems is not free to avoid the heat exchanger entirely as inlet pressure increases.

The current study follows more closely a series of optimization studies that focused on optimizing the geometry of single channels to maximize heat transfer for a specified pressure drop within each channel. Numerous geometric parameters have been optimized in studies of this type including channel width, fin shape (tube, plate, elliptical, etc.) and arrangement of fins within the channel [17–22]. Single channel optimization is a valid surrogate for optimization of an entire heat exchanger when the width of the heat

exchanger is sufficiently large that end effects can be neglected, but the heat exchangers in the current study are specifically those for which this assumption is invalid.

The studies that most closely resemble the present work are those by Bello-Ochende et al. [23] and Bejan and Dan [24]. Both studies, like the current study, sought to maximize heat transfer given and 3-D volumetric constraint and both allowed for the possibility of complex fin geometry. Both, however, also assumed uniform inlet pressure to drive the flow.

This paper presents results for numerical simulations of heat exchangers in low Reynolds number flow that is free to bypass the heat exchanger as a result of the high pressure region that develops at the entrance to the heat exchanger. The overall goal of this project is to find the geometric arrangement of fins that will maximize heat transfer from a given volume. The current work demonstrates that significant increases in heat transfer can be achieved by selective removal of circular pin fins from a standard heat exchanger configuration.

2. NUMERICAL MODEL

This The heat exchanger examined in this study was a tube bank exchanger in crossflow with equilateral triangular fin spacing as illustrated in Fig. 1. This type of heat exchanger was optimized based on an assumption of uniform inlet pressure by Stanescu et al. [18] and the optimal spacing of the fins was shown to be approximated by the expression:

$$(S/D) = 2.2\,\mathrm{Pr}^{-0.13}(D/L)^{-2/5}\,\mathrm{Re}_D^{\,-3/10}, \tag{1}$$

where S is the spacing between tubes as illustrated in Fig. 1, D is the tube diameter, L is the depth of the tube bank (Fig. 1), Pr is the Prandtl number and Re_D is the Reynolds number based on tube diameter.

The heat exchanger was initially modeled containing 18 tubes arranged in an equilateral triangular pattern with S/D = 2. This resulted in a L value of 10D and an H value of 10.39 D.

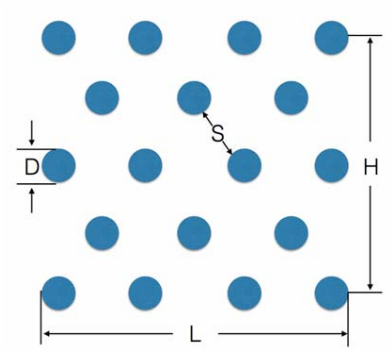

Fig. 1 – Tube bank heat exchanger and relevant dimensions.

The system was modeled as two-dimensional incompressible flow that was weakly coupled to the energy equation. The tubes were considered to be isothermal at a temperature T_H and the inlet flow was modeled as having uniform inlet velocity and temperature: U_0 and T_0. The equations were non-dimensionalised based on U_0, D and the temperature difference T_H–T_0 such that the dimensionless variables were $\mathbf{x}$ = x/D, $\mathbf{y}$ = y/D, $\mathbf{u_1}$ = u/U_0, $\mathbf{u_2}$ = v/U_0, $\mathbf{P}$ = P/(ρ U_0^2) and θ = (T–T_0)/(T_H–T_0), where ρ is fluid density. The governing equations, therefore, were:

$$\mathbf{u}_{i,j} = 0, \tag{2}$$

$$\mathbf{u}_i\mathbf{u}_{i,j} = -\mathbf{P}_{,i} + \frac{1}{\mathrm{Re}_D}\mathbf{u}_{i,i,j}, \tag{3}$$

$$\mathbf{u}_j\boldsymbol{\theta}_j = \frac{1}{\mathrm{Pr}\,\mathrm{Re}_D}\boldsymbol{\theta}_{,j,j}, \tag{4}$$

The main quantity of interest is the total heat flux per unit length of the heat exchanger in the *z* direction: q'. The non-dimensional form of this flux is:

$$\mathbf{Q} = \frac{q'}{\mathrm{k\,Pr\,\Delta T\,Re}_D}, \tag{5}$$

where k is the thermal conductivity of the fluid and $\Delta T = (T_H - T_0)$.

Q was evaluated by integrating the product **u**θ along the flow outlet and results are reported in terms of the ratio (**R**) of the calculated heat flux to the amount of heat flux that would occur if all the fluid that would flow through the area occupied heat exchanger if the heat exchanger were not present, were heated to the wall temperature T_H.

$$\mathbf{R} = \frac{\mathbf{Q}}{\mathbf{Q}_{idealized}}. \tag{6}$$

The system was modeled for $Re_D = 10$ and Pr = 1 because we expect the effect of interest to occur in the low Reynolds number regime. The computational domain is illustrated in Fig. 2. The heat exchange and flow fields are symmetric about the midline of the heat exchanger so only the upper half of the heat exchanger was modeled. The dimensions of the entrance region (EL), exit region (EX) and region of flow above the heat exchanger (OH) were all increased until a further doubling in their size resulted in less than a 1% change in the total heat flux. The values used in simulation were EL = 50 D, OH = 94.5 D and EX = 4 D.

The tubes are numbered in order to identify which tubes are removed during simulations. Boundary conditions on the tube walls were no-slip, no penetration. The top boundary was free slip, no penetration. There was uniform flow at the inlet $\mathbf{u_i}$ = (1,0) and the outflow boundary was modeled with normal derivatives equal to zero at the boundary. Pressure was set to zero at the outlet with derivatives normal to all other surfaces and boundaries set to zero.

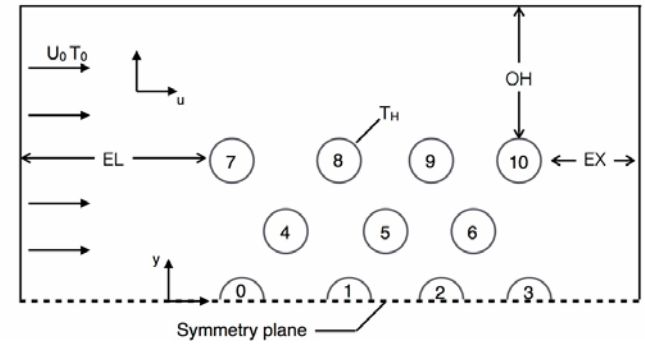

Fig. 2 – The computational domain.

The system of equations 2–4 was solved using the OpenFoam finite element package. The simpleFoam solver was used to find solutions for equations 2 and 3 and the scalarTransportFoam solver was used to solve eq. 5 on a frozen flow field exported from the simpleFoam solution. Convergence testing was performed by decreasing the solver convergence criteria by a factor of 10 until such a decrease led to a less than 1% change in **Q.** Grid convergence was performed by doubling the number of elements in both the x and y direction (increasing elements in the region by a factor of 4) until such doubling resulted in less than a 1% change in **Q**.

A uniform grid was used in all regions except for the y-direction in the OH region, in which a grading ratio of 1:10 was used to put a finer mesh near the tube bank and a coarser mesh near the top of the domain.

3. RESULTS

This Simulations were run for a bank containing all 11 tubes as illustrated in Fig. 2 and then tubes were eliminated to seek configurations that increased **R.** In all there are 2047 possible configurations that include at least one tube out of the 11 possible in the tube bank under study. Work is underway to fully automate the optimization so that all possible configurations of this type can be examined by brute force, but for this preliminary study results were analyzed individually and trends were observed to identify the most productive configuration.

Figure 3 shows the results for the velocity and temperature fields for the bank with all 11 tubes. As anticipated the flow field mostly bypasses the tube bank with velocities over the top of the tube bank reaching about 1.2 U_0 while a large region of very low velocity flow develops within and behind the bank. A corresponding large region of warm fluid develops around the interior and back tubes which, of course, leads to relatively poor heat transfer in these regions.

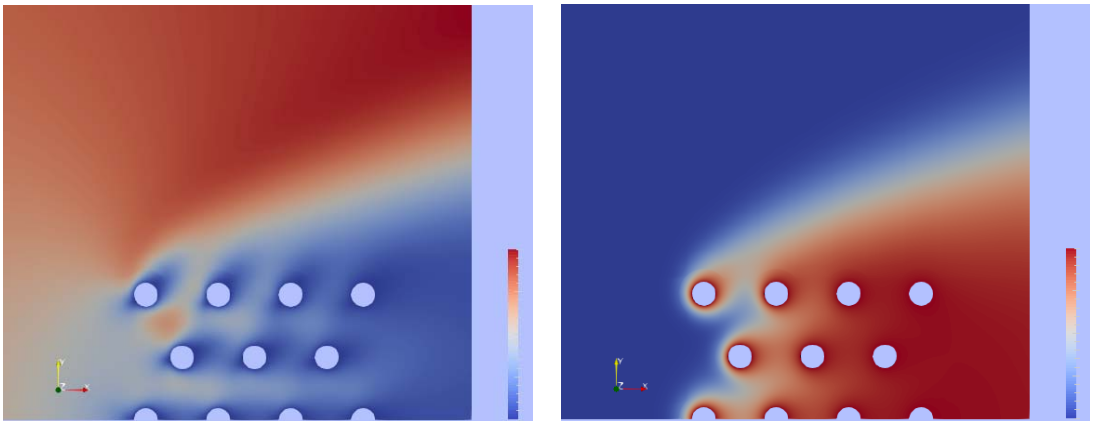

Fig. 3 – Velocity field (left) and theta field (right) with all 11 tubes present. Velocity scale goes from 0 (blue) to 1.2 (red). Theta goes from 0 (blue) to 1 (red).

The optimum configuration for this tube bank under these flow conditions is illustrated in figure 4. In this configuration tubes 0, 1, 4 and 5 have been removed. These results in more flow being forced into the interior of the tube bank and therefore to higher flow velocities within the heat exchanger and a 33% increase in total heat flux compared to the 11 tube configuration.

Removing tubes from the leading edge of the bank near the center of the tube bank provides the greatest increase in heat flux – i.e. removal of tubes 0 and 4. Removal of tube 7, however, which is also located at the leading edge of the tube bank, demonstrates that it is not simply a matter of decreasing the number of tubes that is causing the increase in heat flux, but rather the creation of a geometrical arrangement that promotes flow into the interior of the heat exchanger. The removal of tube 7, the top left most tube, results in a 20% decrease in heat flux compared to the 11 tube configuration, because the removal of that tube creates a leading edge profile that encourages the flow to bypass the heat exchanger and flow over the top of the tube bank.

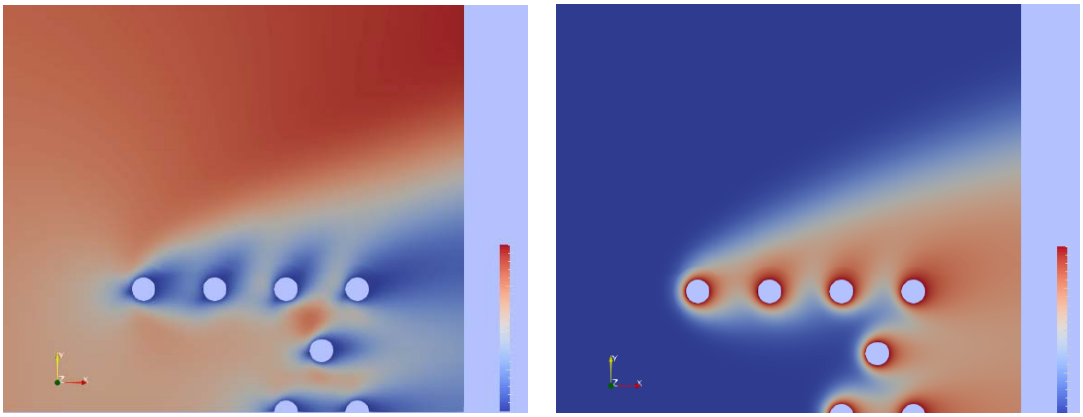

Fig. 4 – Velocity field (left) and theta field (right) for the optimum configuration in which tubes 0,1,4 and 5 have been removed.

Continuing to remove tubes from the leading edge of the tube bank near the center continues to increase the heat flux as more fluid enters the interior of the heat exchanger and fluid velocities near the remaining tubes increase as illustrated in Fig. 4. However, continuing to remove tubes beyond the configuration in Fig. 4 leads to a decrease in heat flux as shown by the last column in table 1 in which the result from the best case for removal of an additional tube is shown.

Table 1

R values for a selection of configurations

Removed tube #s	**R**
None	0.358
0	0.390
4	0.424
7	0.287
0,1	0.432
4,5	0.460
0,1,4	0.465
0,1,4,5	0.477
0,1,2,4,5	0.387

4. CONCLUSIONS

This preliminary study has validated the concept that in the low Reynolds number regime the shape of the heat exchanger can play a significant role in promoting or inhibiting the effectiveness of a heat exchanger. The removal of 4 tubes from the top half of a classic tube bank heat exchanger (or 6 tubes from the whole bank) can lead to significant increase in the overall heat flux, but the selection of which tubes are removed is critical. In general, as expected, removing tubes so as to direct the flow into the center of the heat exchanger rather than around its outside leads to increased heat transfer. Future work will allow for variation in tube diameter, allow the tube positions to become completely flexible within the tube bank and ultimately allow the shape of the heat transfer surfaces to be optimized as well; although it may be expected that for low Reynolds numbers the shape of the surfaces may be unimportant. Finally the study must establish the range of Reynolds and Prandtl numbers for which these geometric considerations are of importance.

REFERENCES

1. GURURATANA, S. *Heat transfer augmentation for electronic cooling*, American Journal of Applied Sciences, **3**, pp. 436–439, 2012.
2. DU, T., DU, W., CHE, K.,CHENG, L., *Parametric optimization of overlapped helical baffled heat exchangers by Taguchi method*, Applied Thermal Engineering, **85**, pp. 334–339, 2015.
3. FETTAKA, S., THIBAULT, J., GUPTA, Y., *Design of shell-and-tube heat exchangers using multiobjective optimization*, International Journal of Heat and Mass Transfer, **60**, pp. 343–354, 2013.
4. GUO, J., CHENG, L., XU, M., *Optimization design of shell-and-tube heat exchanger by entropy generation minimization and genetic algorithm*, Applied Thermal Engineering, **29**, pp. 2954–2960, 2009.
5. GUO, J., XU, M., CHENG, L., *The application of field synergy number in shell-and-tube heat exchanger optimization design*, Applied Energy, **86**, pp. 2079–2087, 2009.
6. MISHRA, M., DAS, P.K., SARANGI, S., *Second law based optimisation of crossflow plate-fin heat exchanger design using genetic algorithm*, Applied Thermal Engineering, **29**, pp. 2983–2989, 2009.
7. MOTA, F., RAVAGNANI, A.S.S., CARVALHO, E.P., *Optimal design of plate heat exchangers*, Applied Thermal Engineering, **63**, pp. 33–39, 2014.
8. PENG, H., LING, X., *Optimal design approach for the plate-fin heat exchnagers using neural networks cooperated with genetic algorithms*, Applied Thermal Engineering, **28**, pp. 642–650, 2008.
9. PONCE-ORTEGA, J.M., SERNA-GONZALEZ, M., JIMENEZ-GUTIERREZ, A., *Use of genetic algorithms for the optimal design of shell-and-tube heat exchangers*, Applied Thermal Engineering, **29**, pp. 203–209, 2009.
10. ROGIERS, F., BAELMANS, M., *Towards maximal heat transfer rate densities for small-scale high effectiveness parallel-plate heat exchangers*, International Journal of Heat and Mass Transfer, **53**, pp. 605–614, 2010.

11. VARGAS, J.V.C., BEJAN, A., *Integrative thermodynamic optimization of the environmental control system of an aircraft*, International Journal of Heat and Mass Transfer, **44**, pp. 3907–3917, 2001.
12. VARGAS, J.V.C., BEJAN, A., *Thermodynamic optimization of finned crossflow heat exchangers for aircraft environmental control systems*, International Journal of Heat and Fluid Flow, **22**, pp. 657–665, 2001.
13. VARGAS, J.V.C., BEJAN, A., SIEMS, D.L., *Integrative thermodynamic optimization of the crossflow heat exchanger for an aircraft environmental control system*, Journal of Heat Transfer, **123**, pp. 760–769, 2001.
14. XIE, G.N., SUNDEN, B., WANG, Q.W., *Optimization of compact heat exchangers by a genetic algorithm*, Applied Thermal Engineering, **28**, pp. 895–906, 2008.
15. ZAREA, H., KASHKOOLI, M., MEHRYAN, A.M., SAFFARIAN, R., BEHEGHANI, E.N., *Optimal design of plate-fin heat exchangers by a Bees algorithm*, Applied Thermal Engineering, **69**, pp. 267–277, 2014.
16. ZHOU, Y., ZHU, L., YU, J, LI, Y., *Optimization of plate-fin heat exchangers by minimizing specific entropy generation rate*, International Journal of Heat and Mass Transfer, **78**, pp. 942–946, 2014.
17. BEJAN, A., MOREGA, A., *Optimal array of pin fins and plate fins in laminar forced convection*, Journal of Heat Transfer, **115**, pp. 75–83, 1993.
18. STANESCU, G., FOWLER, A.J., BEJAN, A., *The optimal spacing of cylinders in free-stream cross flow forced convection*, International Journal of Heat and Mass Transfer, **39**, pp. 311–317, 1996.
19. FOWLER, A.J., LEDEZMA, G.A., BEJAN, A., *Optimal geometric arrangement of staggered plates in forced convection*, International Journal of Heat and Mass Transfer, **40**, pp. 1795–1805, 1997.
20. MATOS, R.S., VARGAS, J.V.C., LAURSEN, T.A., BEJAN, A., *Optimally staggered finned circular and elliptic tubes in forced convection*, International Journal of Heat and Mass Transfer, **47**, pp. 1347–1359, 2004.
21. MATOS, R.S., LAURSEN, T.A., VARGAS, J.V.C., BEJAN, A., *Three-dimensional optimization of staggered finned circular and elliptic tubes in forced convection*, International journal of Thermal Sciences, **43**, pp. 477–487, 2004.
22. WANG, H., LIU, Y., YANG, P., WU, R., HE, Y., *Parametric study and optimization of H-type finned tube heat exchangers using Taguchi method*, Applied Thermal Engineerimg, **103**, pp. 128–138, 2016.
23. BELLO-OCHENDE, T., MEYER, J.P., DIRKER, J., *Three-dimensional multi-scale plate assembly for maximum heat transfer rate density*, International Journal of Heat and Mass Transfer, **53**, pp. 586–593, 2010.
24. BEJAN, A., DAN, N., *Constructal trees of convective fins*, Journal of Heat Transfer, **121**, pp. 675–682, 1999.